Comparison of H_β theory and experiment at electron densities near 10^{15} cm^{-3}†

D. L. Evans*
Mechanical Engineering Department, Arizona State University, Tempe, Arizona 85281

D. P. Aeschliman and R. A. Hill
Sandia Laboratories, Albuquerque, New Mexico 87115

(Received 29 July 1974)

Theoretical H_β profiles by Vidal, Cooper, and Smith (VCS) and by Kepple and Griem (KG), convolved with the appropriate Doppler and instrument widths, have been compared to experimental H_β profiles obtained over the electron density range $4 \times 10^{14} \leq n_e \leq 2 \times 10^{15}$ cm^{-3}. The data were taken in a laminar argon plasmajet seeded with up to 1% H_2. Electron and atom temperatures were $\sim 8 \times 10^3$ and $\sim 6 \times 10^3$ K, respectively. Independent determinations of n_e were based on Stark-shift measurements of the 7273-Å Ar I line using a Fabry-Perot interferometer. Experimental H_β profiles were compared to theory by fitting the logarithms of the intensity by least squares while maintaining profile area normalization to obtain "best-fit" values for n_e. A log fit effectively deweights the points near the line center, where the theoretical accuracy is poor, and thus, compared to a linear fit, yields n_e's in better agreement with the independently determined n_e's. For a given theory, no statistically significant difference was observed between values of n_e obtained using log-profile fitting and half-widths over the n_e range examined—for both methods, $n_e(H_\beta)/n_e$ (7273-Å Ar I) = 0.89 ± 0.20 and 0.80 ± 0.20 for VCS and KG theories, respectively. However, n_e's obtained using the two methods do not necessarily agree on a point-by-point basis. Finally, recent theoretical profiles including ion dynamic effects calculated by Cooper, Smith, and Vidal have been compared to our experimental profiles. Although improved agreement is noted in the vicinity of the line center (shallower theoretical dip-depth), the best-fit n_e's are ~ 10% lower than from VCS theory neglecting ion dynamics.

I. INTRODUCTION

The shape of the hydrogen Balmer line H_β has been widely used and/or investigated as an electron density (n_e) diagnostic in plasmas (for example, see Refs. 1–9). The accuracy of the two most widely used theories for this line [Vidal-Cooper-Smith[10] (VCS) and Kepple-Griem[11] (KG)], at $n_e > 10^{16}$cm^{-3}, has been confirmed to within 5–10% by Wiese *et al.*[6] In addition to their own detailed wall-stabilized arc study, they have performed an exhaustive survey of other published data. Vidal *et al.*[10] indicate that theoretical accuracy should improve to no worse than ± 5% for $n_e \lesssim 10^{15}$ cm^{-3}.

Published research in this latter electron density range is limited. Peacock *et al.*[7] have used a rapid-scan Fabry-Perot interferometer (FPI) to determine the H_β line profile at various times during the afterglow decay of a z-pinch plasma viewed end on. Electron densities, as determined by several independent methods, were compared to Griem-Kolb-Shen[12] (GKS II) theory over the experimental range $10^{14} < n_e < 10^{17}$. Typical data scatter was about ± 25%, with experimental uncertainties increasing toward the lower n_e's because of increasing Doppler contribution and increasing noise. In addition, their comparisons to theory were based on linewidth measurements, a procedure of questionable validity.[10]

Burgess and Cairns,[8] in a study similar to that of Peacock *et al.*,[7] found that although H_β and laser interferometer measurements agreed to within experimental error, the H_β results were consistently below the interferometer results by roughly 10%. Burgess and Mahon,[9] also employing a z-pinch discharge, in pure hydrogen and in a 99.99%-He–0.01%-H_2 mixture, reconstructed the H_β line profile at $n_e = 10^{15}$ cm^{-3} for direct comparison to the theoretical line profile. They observed significant errors in KG theory (no comparison was made to VCS) in the line center in both the pure-hydrogen and helium-hydrogen plasmas, but concluded that general agreement in the line wings was excellent if the experimental and theoretical profiles were area normalized. For the case of the pure-hydrogen plasma, large corrections for self-absorption were required; hence, although the corrected experimental H_β profile appeared to match the normalized theoretical profile in the wings, the agreement may be spurious. For the seeded helium plasma, the experimental H_β profile appears to deviate by up to 30% in the wings; hence, the claimed agreement between KG theory and the experiment in the line wings would not appear to be justified.

Thus, it appears there has been no adequate test of either VCS or KG theory at $n_e \approx 10^{15}$ cm^{-3}. In this paper, data obtained on a hydrogen-seeded argon plasmajet operating in the range $4 \times 10^{14} < n_e < 2 \times 10^{15}$ cm^{-3} are presented for such a test.

In addition to these results, data based on an analysis of H_β line profiles obtained by Chester and Bengtson[13] in a z-pinch discharge over the range $2.8\times10^{14} \leq n_e \leq 8.0\times10^{14}$ cm^{-3} are presented. A single result based on the H_β profile from the seeded helium plasma of Burgess and Mahon[9] is also included.

It should be noted that most previous authors made comparisons between experiment and theory at the independently measured electron densities, instead of using comparisons between experiment and theory in some best-fit least-squares sense to obtain electron density.[14] The former case is perhaps of greater interest to theoreticians in further development of the theory; the latter approach is of greater interest to those who wish to use the theory in conducting plasma diagnostics. Here, results are presented from both points of view.

II. EXPERIMENT

The plasma source for the present study was a Plasmadyne arc heater operated between 1000- and 2000-A dc depending on the desired electron density. A contoured convergent-divergent nozzle of exit diameter 3.18 cm was used to produce a radially symmetric, parallel, field-free plasma. Exit velocities were typically 3.0×10^5 cm/sec. Measurements were conducted 3.2-cm downstream of the nozzle exit after a prior investigation demonstrated that axial gradients were negligible. Test-chamber pressures between 8.5 and 18 torr, depending on plasmajet operating conditions, were balanced with nozzle-exit pressures so as to prevent shock formation in the flow.

A small amount of hydrogen, 0.15 to 1% by volume, was mixed with the argon working gas upstream of the arc heater. Argon flow rates were typically 1.8 to 4.0 g/sec. In all cases the seed ratios were sufficient to yield peak H_β-line signal-to-noise ratios of better than 50:1. With no hydrogen flow, the spectrum in the vicinity of H_β was devoid of any structure other than a constant continuum attributable to argon, and a very weak H_β line, due to the $\leq 0.01\%$ water-vapor impurity in the bottled argon gas used.

Figure 1 shows a schematic of the experimental system. The jet was viewed at $\theta = 56.5°$ (a convenient angle for Doppler-shift measurements) through a schlieren quality window by a scanning mirror. This mirror was driven about a horizontal axis by a reversible synchronous motor to produce lateral scans of the jet. Data acquisition was automated so as to minimize data recording time and human error. The data were recorded directly on magnetic tape by a Honeywell DDP116 computer which was synchronized with the experiment.

A. H_β measurements

The H_β line profiles were investigated using the by-pass beam,[15] BPB (interferometer blocked off), to the $\frac{3}{4}$-m Czerny-Turner monochromator. Entrance and exit slit widths were 20 μm, which produced a nearly Gaussian instrument function (full half-width of 0.28 Å). A spatial resolution in the jet of about 0.8 mm was obtained by limiting the vertical height of the entrance slit to 0.4 mm. A cooled, electrostatically and magnetically shielded EMI 9658R photomultiplier (S-20 spectral response) served as the radiation detector.

The data acquisition and reduction procedures were similar to those used by Popenoe and Shumaker.[1] Typically, 50 lateral scans of the jet were taken at fixed wavelengths separated by 0.215 Å. During an arc traversal, 120 intensities were recorded at 14 msec intervals, corresponding to spatial separations of 0.0254 cm. The continuum background was approximated by taking two oppositely directed lateral scans of the jet at a wavelength -12 Å from the line center (measurement of the continuum at a wavelength +12 Å from the line center agreed to within a few percent). The data were subtracted, point by point, from all the data recorded in the same scan direction for the line plus continuum.

The center of the spatial intensity distribution was determined, and the data were folded about that centerline, smoothed and inverted by the Abel method to radial distributions as is common in axisymmetric arc work.[1,6,16] Porter's method[17] was used for performing the Abel inversion. In the numerical smoothing routine, a tolerance of 2% of the peak intensity was applied. Varying the tolerance over the range 0.25 to 4.0% resulted in less than a 1% effect on the values of n_e obtained by profile fitting (described in Sec. III) for most radii. Figure 2 shows an example of typical H_β data before and after invasion. (The slight peak at $r = 0$ is due to inversion inaccuracies.) The line profile at each radial point was assembled by collecting the appropriate data from each of the wavelengths investigated. Figure 3 shows a typical H_β line profile.

B. Independent n_e measurements

Independent electron density determinations for the flow were based on 7273-Å Ar I Stark-shift measurements. The Stark-shift parameter d (the shift in Å per electron e) employed for the 7273-Å Ar I line was based on line-shift data obtained by Evans and Marchand[18] using a free-burning arc (0.5 to 3.0 atm), and on recent theoretical calculations by Barnard.[19] Evans and Marchand obtained $d = 3.9 \times 10^{-18}$ Å/e over the range 6.0×10^{16} to 5×10^{17}

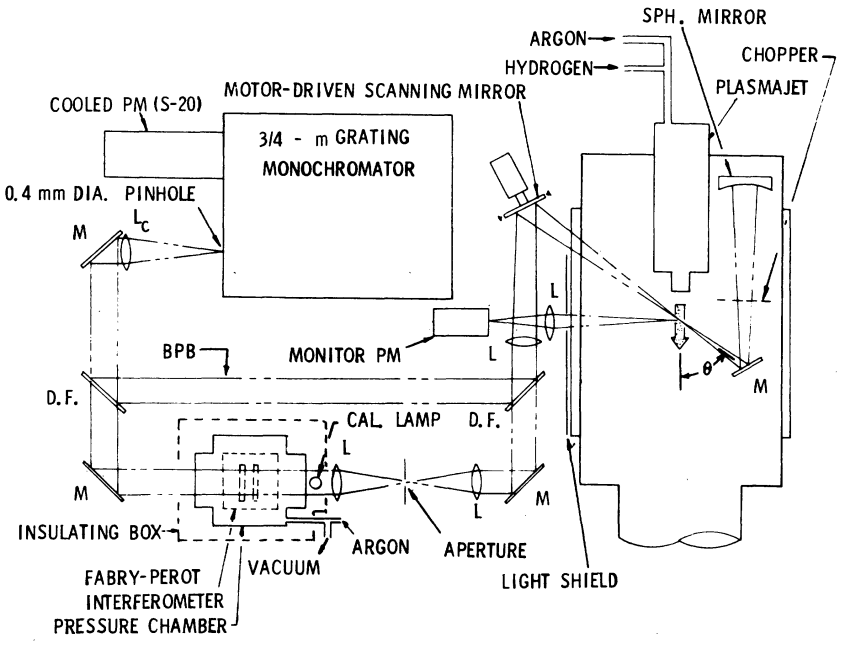

FIG. 1. Schematic of the experimental system. (L, lens; M, plane front-surface mirror; D. F., plane dichroic filter; BPB, by-pass beam.)

cm^{-3}, at electron temperatures of 12 000–16 000 K. Their data, shown in Fig. 4, have typically an uncertainty of about ± 10%. Barnard included Debye shielding effects and both upper- and lower-state perturbations, and obtained $4.1\times10^{-18} \geq d \geq 3.9\times10^{-18}$ Å/e over the same T_e and n_e ranges. (By contrast, Griem,[20] neglecting lower-state perturbations, obtained 8.1×10^{-18} Å/e for the 7273-Å Ar I line.) Barnard's calculations, for which no error estimates are given, indicate that d decreases slightly with increasing T_e and n_e over the ranges $0.8\times10^4 \leq T_e \leq 1.6\times10^4$ K, $10^{14} \leq n_e \leq 5\times10^{17}$ cm^{-3}. In view of the agreement between experiment and theory over the experimental range noted above, the average of the experimental d values and Barnard's predicted dependence of d on T_e and n_e have been used to obtain $d = 4.1\times10^{-18}$ Å/e for the present experiment, for which $7\times10^3 \leq T_e \leq 9\times10^3$ K, $4\times10^{14} \leq n_e \leq 2\times10^{15}$ cm^{-3}.

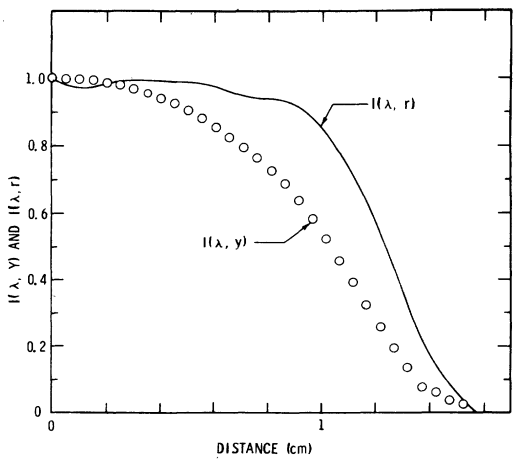

FIG. 2. Lateral and radial distributions (before and after inversion) of relative H_β intensity at $\lambda = -0.7$ Å from the line center in a 2000-A argon plasmajet seeded with 0.15% H_2.

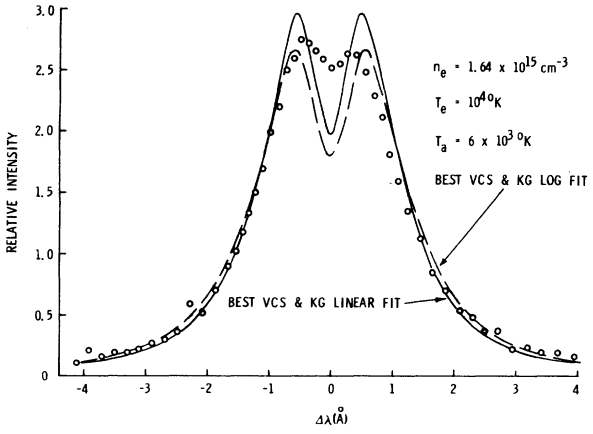

FIG. 3. Typical experimental H_β line profile, in relative intensity units, for a 2000-A argon plasmajet seeded with 0.15% H_2, at an independently measured electron density of $(1.64 \pm 0.30)\times10^{15}$ cm^{-3}. Broken lines, VCS ($n_e = 1.57\times10^{15}$ cm^{-3}) and KG ($n_e = 1.44\times10^{15}$ cm^{-3}) best logarithmic fit; solid lines, VCS ($n_e = 1.34\times10^{15}$ cm^{-3}) and KG ($n_e = 1.23\times10^{15}$ cm^{-3}) best linear fit. Theoretical profiles have been convolved with an instrument and Doppler profile of total width 0.39 Å. Radial position is $r = 0.508$ cm.

A Fabry-Perot interferometer (FPI) was used to obtain the high spectral resolution required for the shift measurements. The FPI plates were enclosed in an invar holder of 55-mm clear aperture; this holder was mounted in a thick-walled brass cylinder which could be evacuated and which permitted external adjustment of the plate parallelism. To isolate the FPI from possible temperature variations over typical run times (10–20 min), the assembly was enclosed in an insulated chamber. The parameters describing the FPI are presented in Table I.

The center of the interference pattern of the jet radiation was focused on a 400-μm-diam pinhole that served as the entrance aperture for the monochromator (BPB blocked). With an exit slit width of 400 μm, the monochromator provided a total spectral bandpass of about 5 Å which served to eliminate unwanted spectral lines. Radiation from higher orders from the 1200-lines/mm grating was removed with a high-pass optical filter.

In the manner of Jacquinot and Dufour,[21] spectral scanning was controlled by varying the pressure (and thus the index of refraction) of the argon gas in the FPI housing. The pressure was measured with a precision strain-gage transducer and recorded on the data tape, with direct readout also available on one channel of a two-pen strip chart recorder. These pressures were converted to wavelengths by scanning the Ar I 7272.94-Å line from an argon Geissler tube (calibration lamp) located in the collimated beam inside the insulated chamber. This permanent position of the calibration lamp avoided the problem of repositioning the lamp at the aperture prior to each run, and the resulting wavelength variations due to variations in the lamp position. This uncollimated illumination of the FPI, however, results in a net line shift of the calibration line that must be measured. Thus, the wavelength emitted by the calibration lamp was compared to that of a variable-pressure argon discharge tube, positioned at the aperture, over a range 1–30 torr. The gas temperature in the variable-pressure lamp was measured with an electrically-floating thermocouple located on the discharge axis. At each of seven different pressures, the emission line was scanned twice with the FPI, and the profile intensities were recorded. Similarly, a total of eight scans of the calibration lamp were made before and after recording the variable-pressure data. All line profiles were least-squares fitted to a Voigt profile whose (small) Doppler component at the calibration wavelength corresponded to the measured gas temperature. The wavelengths of the resulting line centers, relative to the calibration lamp, are shown as a function of argon number density in Fig. 5 for a typical calibration run. An average intercept of −0.0016 Å, with a maximum deviation of 0.0003 Å, was obtained from seven calibration runs taken over a period of several weeks.

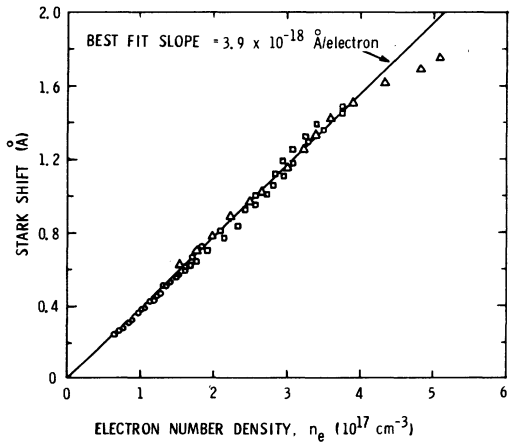

FIG. 4. Stark shift of the 7273-Å Ar I line versus electron density in a free-burning arc over the ranges $0.6 \times 10^{17} \leq n_e \leq 5 \times 10^{17}$ cm^{-3}, $1.2 \times 10^4 \leq T_e \leq 1.6 \times 10^4$ K. Data are from Ref. 18.

The optical system employed a technique described by Aeschliman and Hill[22] to measure both the Doppler and Stark shifts. A spherical mirror (see Fig. 1) is oriented in the test chamber with its optical axis coincident with the optical axis of the interferometer and with its center of curvature at the centerline of the flow. Blue-shifted radiation returned by the spherical mirror is periodically chopped; thus, both Doppler red- and blue-shifted line profiles are recorded in one spectral scan.

In a manner similar to that used to obtain the H_β intensities, lateral scans were taken for typically 30 wavelength increments throughout one

TABLE I. FPI parameters (λ = 7273 Å).

Diameter	60.0 mm
Clear aperture	55.0 mm
Thickness	15.0 mm
Flatness	λ/200
Wedge	0.5°
Coating	Multilayer dielectric
Spacing	10.36 mm
Reflectivity	>99%
Transmission	0.2%
L_c focal length (see Fig. 1)	330 mm
Measured finesse	66

free spectral range (0.255 Å at 7273 Å); 120 intensities were recorded per scan across the jet. These data consisted of alternating chopper-closed (red-shifted) and chopper-open (superposed red- and blue-shifted) intensity values. The data were interpolated, subtracted appropriately, folded about the jet axis, smoothed and inverted by the Abel method to obtain radial distributions. The resulting Doppler red-shifted and blue-shifted spectral lines were reconstructed at each radial point and are shown in Fig. 6. The midpoint between the red-shifted and blue-shifted line centers is the wavelength of the Stark-shifted line. The Stark shift is the difference between the midpoint wavelength and the corrected wavelength of the line from the calibration lamp decreased by a small amount proportional to the argon-atom number density in the jet. Systematic uncertainty in Stark-shift measurement from all sources of error is estimated to be $< \pm 0.0005$ Å. For the conditions of this experiment, this uncertainty leads to possible systematic errors in electron density of 5–10%.

To increase the accuracy of locating the midpoint wavelength, both the red-shifted and blue-shifted lines were fitted, in a least-squares sense, with a theoretical Gaussian line profile given by

$$j_i^c = 2(ln2/\pi)^{1/2} A(\exp\{-2(ln2/\pi)^{1/2} \times[\lambda_i - \lambda_0(r)]^2/\Delta\lambda_D(r)\}\}/\Delta\lambda_D(r),$$

where j_i^c is the calculated monochromatic emission coefficient at the ith wavelength λ_i, where a measurement was made. Here, the line center λ_0, the line (full) half-width $\Delta\lambda_D$, and the constant A were adjusted so as to minimize the sum of the squares of the residuals.

In addition to providing a measurement of the Stark shift (and thus n_e), this procedure also yielded[23] velocity U (from the Doppler shift and angle θ), heavy-particle temperature T_h (from the Doppler contribution to the line half-width), and atom density n_a (from Dalton's law and the perfect-gas equation of state). Electron temperature was determined by means of a Boltzmann plot on the calibrated intensities of Ar I spectral lines originating from upper states of energy 13.33 to 15.13 eV. Within the uncertainties in the transition probabilities (typically ± 20%), and the calibration and inversion errors, these data fit a straight line corresponding to an electron (excitation) temperature $T_e = 8200 \pm 800$ K in the vicinity of the jet axis. Equality of electron and excitation temperature (i.e., the existence of a Boltzmann distribution of excited states at the electron temperature) under similar argon-plasmajet operating conditions has also been observed by Adcock,[24] among others.

Knowing T_e, T_a and n_a were determined in an iterative scheme which accounted for Stark, instrument, and neutral broadening of the atom line, where the Stark-broadening parameter was taken from Ref. 18. Figures 7(a) and 7(b) show the radial distribution of the flow properties, including

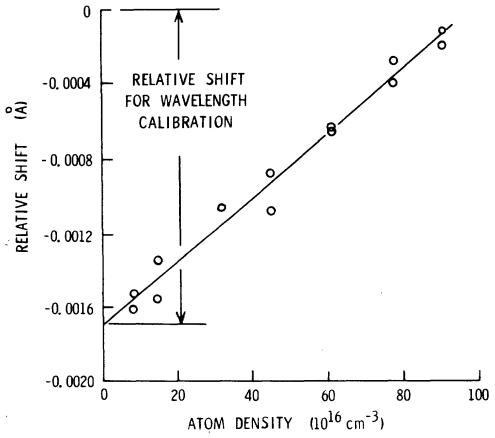

FIG. 5. Shift of the 7273-Å Ar I line emitted by a 3-mm-i.d. variable-pressure lamp with respect to that emitted by the calibration lamp, as a function of atom density in the variable-pressure lamp.

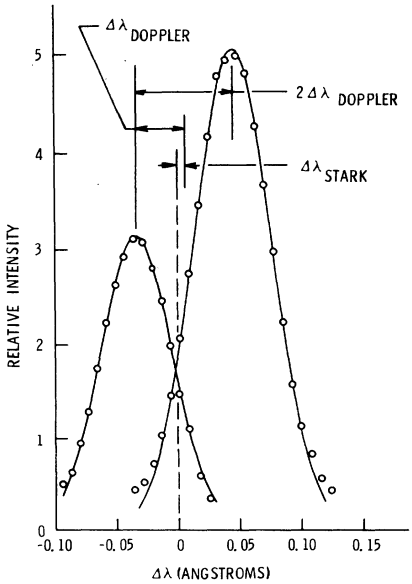

FIG. 6. Typical Doppler red-shifted and blue-shifted 7273-Å Ar I lines at jet conditions of Fig. 3. Blue-shifted peak intensity is reduced owing to additional reflection losses. Line centers are based on least-squares Gaussian fits (solid lines) to the profiles. The jet neutral-atom contribution to the net line shift (~0.0005 Å) is not distinguishable in this plot.

Mach number and enthalpy, for the 2000-A plasmajet seeded with 0.15% H_2.

The H_β- and the argon-line data were recorded on the same jet but were separated slightly in time owing to the double use of some instrumentation. During this time, important arc parameters were monitored and held constant, to within a few percent. The jet total radiation was continuously monitored by means of a 1P21 photomultiplier ("Monitor PM" in Fig. 1), in order to evaluate both short-term fluctuations and long-term drift. For small changes, the monitor was used to adjust the data in order to approximate a constant jet. The average monitor level during a particular scan was ratioed to the average level obtained during the first scan of a data run. All intensity data in the given scan were scaled by the inverse of this ratio, typically 0.97–1.03, in order not to introduce artificial asymmetries into the spectral line profiles. If fluctuations or drifts exceeded 20 and 10%, respectively, the data were discarded.

The monitor signal level is primarily due to continuum radiation, and thus is proportional to $n_e^2/\sqrt{T_e}$. T_e has been observed to be essentially independent of plasmajet operation (< 1% change in T_e for a > 10% change in arc current). Hence, the ratio of average electron density over two consecutive data runs (a total elapsed time of about 10 min) was taken to be the square root of the average monitor level for the two runs. It is emphasized that these were small corrections, typically involving the square root of the intensity ratios noted above.

In support of the method described above, n_e was also obtained from absolute argon continuum measurements on the 2000-A plasmajet; agreement with Stark shift measurements was better than 10%. The Stark-shift and continuum measurements were necessarily carried out in pure argon, using a quantum-mechanical continuum correction factor of 2.5 at 5535 Å.[18]

III. H_β LINE FITTING

Previous investigations have shown the largest deviation between experiment and theory for H_β to be in the immediate vicinity of the line center; the present study offers no exceptions. All theories have, thus far, predicted a much deeper central dip than is actually noted. This large localized discrepancy introduces a serious difficulty if one attempts to determine n_e by comparing an experimental profile to theory in some best-fit manner. Any electron density over a wide range can be found, depending on how the data are weighted, e.g., by assigned weighting functions in the fit or by the distribution of experimental wavelength increments. For example, if one follows the line-fitting technique of Popenoe and Shumaker[1] but ensures area normalization, the best-fit number density for any particular experimental profile continuously increases as more and more of the central wavelength points are excluded from the fit. However, if one uses equally spaced wavelength increments and fits, in a least-squares sense, the *logarithm* of the experimental intensity with the *logarithm* of the H_β theoretical intensity, this problem is alleviated. The weighting accomplished by this technique reduces the effect of the few large residuals near the line center in such a way that the "best" n_e does not change appreciably when central points are omitted from the fit. A comparison of the two fitting techniques is shown in Fig. 3.

Thus, the experimental line profiles are compared with VCS and KG theories by fitting the ln of the experimental intensity j_i^m, at each observed wavelength λ_i with the ln of the theoretical line intensity, given by

$$j_i^t = BS(\alpha).$$

Here, $S(\alpha)$ is the theoretical hydrogen H_β line shape, B is an area scaling factor, and $\alpha = 1.25 \times 10^{-9} |(\lambda_i - \lambda_0)| n_e^{-2/3}$. An iterative technique was used to vary n_e and the line center λ_0 if desired, so as to minimize the function

$$\sum_i (\ln j_i^m - \ln j_i^t)^2$$

within some preset small tolerance. Within each iterative step, B was set equal to the ratio of the area under the measured line, between the highest and lowest wavelength points observed, to the area under the theoretical $S(\alpha)$ profile for the same wavelength (or α) interval.

For both VCS and KG data, $S(\alpha)$ values at $T_e = 10^4$ K and $n_e = 10^{14}$, $10^{14.5}$, 10^{15}, $10^{15.5}$, 10^{16} have been folded with a Gaussian slit width of 0.28 Å (full half-width) and a Doppler width corresponding to an atom temperature of 6000 K (see Fig. 7).[25] The logarithms of these five sets of $S(\alpha)$'s were fitted piecewise by cubic equations in α in all the VCS tabulated α intervals over the range $0.001 \leq \alpha \leq 6.31$ (the upper limit was chosen to permit analysis of the data of Chester and Bengtson[13]; for our data, $\alpha < 0.4$). For the interval $0 \leq \alpha \leq 0.001$, a parabola has been used with the condition $dS/d\alpha = 0$ at $\alpha = 0$.

Since the tabulated α values are different for KG, a rigorous interpolation of their data has been carried out in order to give the same α intervals as VCS. This necessitated interpolation within the KG tables for $0 \leq \alpha \leq 0.35$ and the use of the KG modified wing formula[11] for $0.35 \leq \alpha \leq 1.05$.

For $1.05 \leq \alpha \leq 6.31$ we have attached a pure $\alpha^{-5/2}$ (Holtzmark) wing matched to the modified wing formula at $\alpha = 1.05$.

In use, the line-fitting routine iterates from initial estimates of n_e and λ_0 to the values yielding the best fit, each time using the set of cubic coefficients that correspond to the line shape at the nearest tabulated n_e; this procedure adequately accounts for the small dependence of $S(\alpha)$ on n_e. Because of area normalization between the measured profile and the corresponding (symmetric) theoretical profile, the resultant line center was shifted slightly toward the blue (because of the higher blue wing peak) and thus tended to mask genuine line asymmetries. However, the shifts were less than the H_β Doppler shifts (~0.03 Å) and thus introduced negligible error in the fitting routine.

Figure 8 shows typical results obtained by using the two techniques of fitting either the intensities, or the logarithms of the intensities. The abscissa of this figure is the fractional intensity, based on the peak height, of the line profile above which all points were discarded from the fit.

Another program option permitted the computation of the theoretical profile corresponding to fixed values of n_e and λ_0. The former was the independently determined n_e from the 7273-Å Ar I Stark-shift measurements, corrected for monitor drift as mentioned above; the latter was normally that determined by a least-squares fit to the experimental H_β profile.

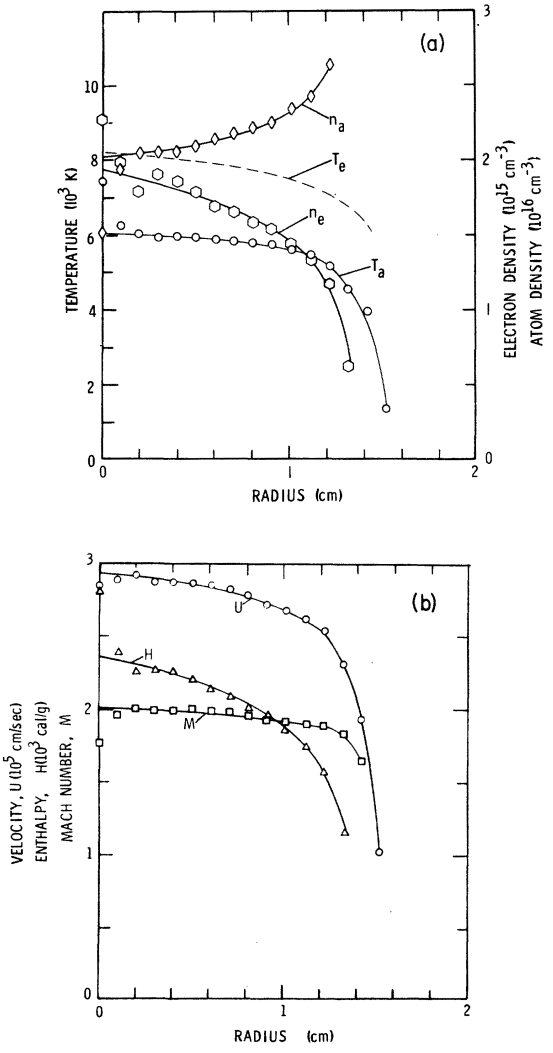

FIG. 7. Radial distributions of flow properties in 2000-Å argon plasmajet seeded with 0.15% H_2. Jet static pressure is 18 torr; arc voltage is 40.0-V dc. (a) Stark-shift based electron density n_e, atom density n_a, electron temperature T_e, and atom temperature T_a. (b) Velocity U, enthalpy H, and heavy-particle Mach number M. Deviations near jet axis are due to Abel inversion technique.

IV. RESULTS AND DISCUSSION

A. Whole-line fitting to determine n_e

The independently determined n_e for the data shown in Fig. 3 is $1.64(\pm 0.30) \times 10^{15}$ cm^{-3}. It can be seen that the blue wing peak intensity exceeds the red wing peak intensity. This trait characterized all of our data where separate peaks were distinguishable (at the lower values of n_e the peaks merge and become indistinct) as well as the data of nearly all other investigators, with the possible exception of Burgess and Mahon.[9]

Shown in Fig. 3 are the best-fit VCS theory and the best-fit KG theory that resulted from fitting the logarithm of the intensities. To the accuracy that can be shown on that plot, there was no difference in the "best-fit" line profile between VCS and KG

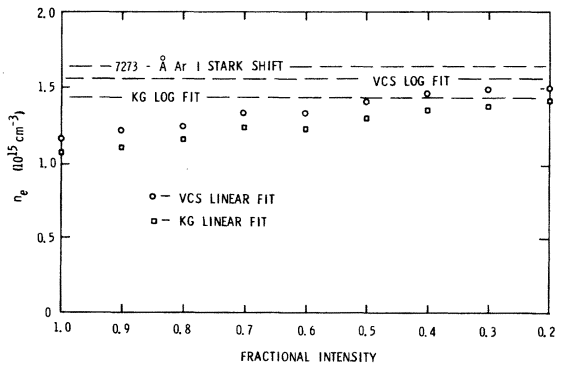

FIG. 8. Electron densities obtained from the H_β profile of Fig. 3 using least-squares line-fitting method with area normalization versus H_β line fractional intensity (see text) for both logarithmic and linear fits. "Log-fit" results are independent of fractional intensity.

theory. Both theories had an rms relative deviation, based on the natural logarithms of the intensities, of 0.157, which translates into an average percent error over the profile[26] of 17%. However, the n_e's corresponding to the logarithmic fits were 1.57×10^{15} cm^{-3} for VCS and 1.44×10^{15} cm^{-3} for KG. This difference of nearly 10% was typical of that observed in all our data.

Fitting the intensities instead of the logarithms of the intensities also yielded identical best-fit *line profiles* for both theories but with different number densities, 1.34×10^{15} cm^{-3} for VCS and 1.23×10^{15} cm^{-3} for KG. The average percent error over the profile for this type of fit was 23% for both theories. Figure 3 also shows the results of these "linear" fits.

The results of this experiment for $0.3 \leq r \leq 1.2$ cm are displayed in Fig. 9, which shows the n_e determined from Stark-shift measurements versus the best-fit (ln of the intensities) n_e with VCS theory. The solid curve represents a first-order least-squares fit for the data shown; its slope is 0.89. Data obtained using KG theory are not shown in Fig. 9; the best fit for the KG comparison has a slope of 0.80. Also not shown are the least-squares fits to the data obtained using linear fits; the slopes of these lines are 0.76 and 0.68 for the VCS and KG theories, respectively. The horizontal error bars attached to the solid line represent the bounds on our possible systematic errors. These bounds include the effects of a ± 10% possible uncertainty in Stark-shift parameter, inversion errors, and estimates of possible errors due to absorption and Stark-shift calibration.

Calculations have shown that the small amount of absorption which may be present should not affect the hydrogen profiles to any significant degree. However, small amounts in the argon line are significant in the Stark-shift measurements since the blue-shifted line makes an additional pass back through the plasma. Thus, the red side of the blue-shifted argon line (see Fig. 6) may be absorbed by up to 3% near the half-intensity point. This should cause the Stark-shift-determined n_e's to be low by 5% or less.

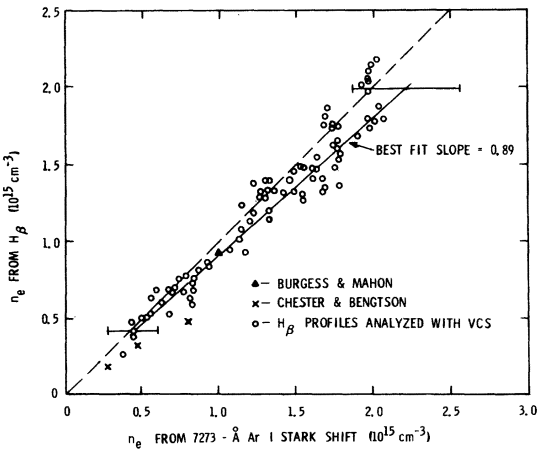

FIG. 9. n_e from VCS log fits to experimental H_β profiles versus 7273-Å Ar I Stark-shift-based n_e. Dashed line represents perfect agreement. Solid line represents a least-squares-fit slope of 0.89 for VCS log fits. Slope of 0.80 for KG log fits is not shown.

Calibration errors for the Stark shift consist of a possible ± 0.0005-Å systematic error and a possible ± 0.0005-Å random run-to-run variation. The former does not affect the slope of the solid line in Fig. 9. The run-to-run variations lead to an uncertainty in the slope of about ± 5%. Finally, errors in the Stark shift associated with the Gaussian fits to the individual argon line profiles are ± 5 to ± 10% and are random.

Analyses of the data of both Chester and Bengtson[13] and Burgess and Mahon[9] have been carried out with the result that the best-fit n_e's are lower than their independently determined n_e's. The results of these comparisons are shown in Fig. 9 using their independently determined n_e's as the abscissa.

Electron densities obtained using the logarithmic fit to the H_β profiles of Chester and Bengtson, especially at 8×10^{14} cm^{-3}, are 20–40% lower than the present data, although the exact cause of this remains unexplained at the present time. Part of this could be due to differences in the plasma source and/or operating parameters.[27]

The data of Burgess and Mahon, [9] taken at equal wavelength increments from their published curves for the 99.99%-He–0.01%-H_2 mixture yield a best-fit n_e in excellent agreement with the present results. It is interesting to note that both experiments[9,13] cited above have used z-pinch discharges of comparable lengths but widely different diameters and initial fill pressures.[28] Chester and Bengtson[13] used pure hydrogen and observed significant self-absorption in the central part of the line. They applied corrections of up to 58% to their H_β profiles. Data taken in the admixture used by Burgess and Mahon[9] required no corrections for absorption.

As noted in Sec. III, the largest discrepancy between theory and experiment occurs in the central-dip region. Hill, Gerardo, and Kepple[29] have suggested that ion dynamics might account for these discrepancies. Relative motion between ions and radiating atoms, which is absent from the theory, should tend to fill in the deep central dip predicted by both VCS and KG. In a recent paper, [30] Kelleher and Wiese have experimentally shown that, indeed, the relative dip scales inversely with the square

root of the reduced mass, a result that might be expected from ion dynamic effects.

Recent work by Cooper *et al.*[31] incorporates ion dynamics into previous theory[10] with the assumption that strong ion-radiating atom collisions are separated in time. They present calculations in the n_e range 10^{13}–10^{15} cm^{-3} with the caution that the above assumption is of marginal validity at the higher end of that range.

Figure 10 shows the data of Fig. 3 compared to the new theory[31] for an ion-atom reduced mass of 0.975 (the reduced mass for a hydrogen-argon collision) and a heavy-particle temperature of 6000 K. Although the predicted central dip is relatively smaller than that for VCS theory, in closer agreement with experiment, the best-fit n_e with ion dynamics is much lower. Analysis of the Burgess-Mahon data shows a similar trend; the best-fit n_e drops from 9.2×10^{14} to 7.7×10^{14} cm^{-3}.

At lower densities [$(2-4)\times10^{14}$ cm^{-3}], where the new theory predicts no central dip and where the assumptions inherent in it should be more applicable, the trends are similar; the best-fit n_e's are systematically lower with ion dynamics than without. The source of this discrepancy is at present unexplained.

B. Use of half-widths to determine n_e

Although Vidal *et al.*[10] have cautioned against use of fractional widths to determine n_e, this procedure has been and will probably continue to be a widely used technique. Its ease of application is its most favorable attribute. The half-width, based on a maximum intensity determined from the average of the red and blue peaks of H_β, is the most commonly used of the fractional widths.[3,5]

In Fig. 11, the Stark-shift-based electron densities are compared with electron densities determined from VCS half-widths interpolated from their tables after folding with the appropriate Doppler and instrument widths. The solid curve represents the best straight-line fit to that data and has a slope of 0.89. As in the case of whole-line fitting, n_e's based on KG theory consistently fall about 10% below the VCS results. The best straight-line fit to the KG data has a slope of 0.80.

C. Comparison at a known n_e

As explained in the Introduction, it is perhaps instructive in the development of the theory to compare the theory at some n_e with a measured profile at that same density. This has been done in Fig. 12, where the data of Fig. 3 are compared to the area-normalized VCS and KG theories at $n_e = 1.64\times10^{15}$ cm^{-3}. The average percent error over the profile was 18% for the VCS theory and 23% for the KG theory. This is typical of all our data.

V. CONCLUSIONS

It is important to note that electron densities determined by comparing experiment with theory depend upon how that comparison is made. In the present electron density regime, fitting the logarithms of the measured intensities with the area-normalized VCS theoretical profiles appears to

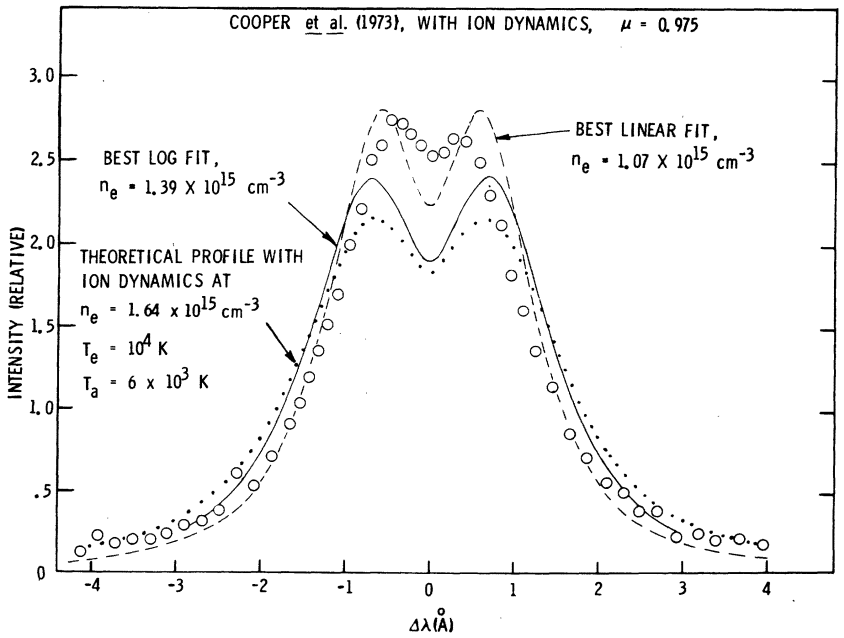

FIG. 10. Ion dynamics theory of Cooper, Smith, and Vidal (Ref. 31) for a reduced mass of 0.975 compared to the experimental data of Fig. 3. Curves: dotted line, theoretical profile with ion dynamics at $n_e = 1.64\times10^{15}$ cm^{-3}; solid line, best log fit; broken line, best "linear" fit; circles, experimental intensities at $n_e = 1.64\times10^{15}$ cm^{-3}.

give the best results in that, although consistently low, they fall within our estimated experimental error. KG theory, used in the same manner, appears to yield electron densities that on the average are at the extreme lower bound of our estimated experimental error.

For all profiles analyzed by fitting the intensities (as opposed to the logarithms of the intensities), electron densities obtained using both VCS and KG theory fall out of range of the estimated experimental error. Again, KG results consistently lie below VCS theory by typically 10%. The data of other investigators[8,9,13] tend to support the above conclusions.

As noted above, the agreement between theory and experiment, as defined by least-squares straight-line fits to the n_e-vs-n_e data (Fig. 9 and 11), appears to be as good for half-width-based n_e's as for results obtained from full-profile log fitting. It is stressed, however, that this agreement does not hold on a point-by-point basis, i.e., the electron density derived from the half-width of any given profile may be larger or smaller than n_e based on a "logarithmic" best fit to the whole line profile. This result is not explained, although it may be due, at least in part, to inaccuracies inherent in the establishment of the effective profile peak height in the presence of merging red and blue peaks.

As noted in Sec. IV, absorption in the 7273-Å Ar I line could affect our results slightly; this effect is not included in the data of Fig. 9 and 11. Correction for absorption would shift the independently determined n_e's to the right by no more than 5%, and thus increase the difference between theory and experiment. Also, the use of 3.9×10^{-18} Å/e instead of 4.1×10^{-18} Å/e for the Stark-shift parameter (see Sec. IIB) would move the data to the right on Figs. 9 and 11, again increasing the apparent discrepancy between theory and experiment.

Because of the possibility of macroscopic fluid turbulence and its effect on line broadening,[20] some discussion of this subject is perhaps in order. Although the plasma velocity is high ($\sim3\times10^5$ cm/sec), the Reynolds number for the flow is only about 2000 for the central portion of the jet and rises to about five times that on the outer periphery. This is based on the diameter of the nozzle exit (and coincidentally, on the distance downstream from the exit) and on the viscosity measurements of Aeschliman and Cambel.[32] Reynolds numbers of about 10^5 are necessary for transition to turbulence,[33] an estimate that has been essentially confirmed by Demetriades and Doughman,[34] who have observed transition to turbulence in a similar jet at a distance of about 40-cm downstream from the nozzle.

To provide data in a form typically utilized by theorists, we have also compared theoretical and experimental H_β profiles at the independently determined number density. It was found that VCS offers a smaller average percent error over the profile. In view of our possible experimental errors, it is not certain that VCS theory is superior to KG theory; however, the data of Burgess and Mahon,[9] and Chester and Bengtson[13] support the present results.

It is concluded that more work on the theoretical profiles is necessary to bring them in closer agreement with experiment, particularly in the vicinity of the line center.

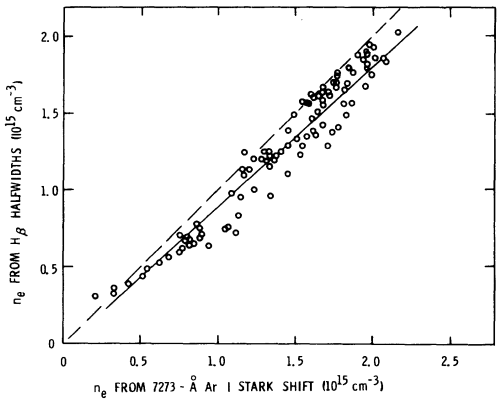

FIG. 11. VCS H_β-half-width-based n_e versus 7273-Å Ar I Stark-shift-based n_e. Dashed line represents perfect agreement. Solid line represents a least-squares-fit slope of 0.89. Slope of 0.80 for KG H_β-half-width-based n_e is not shown.

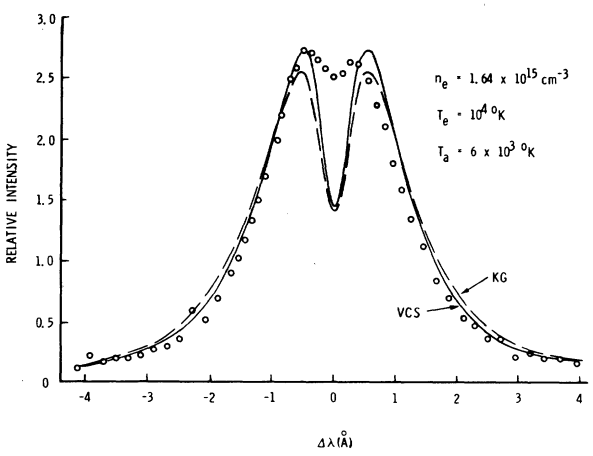

FIG. 12. Comparison of experimental H_β profile and area-normalized VCS and KG theoretical profiles at $n_e = 1.64\times10^{15}$ cm^{-3}.

ACKNOWLEDGMENTS

The authors gratefully acknowledge the aid of G. A. Arnot, D. E. Berg, and D. R. MacKenzie with the computer/experiment interface, and W. H. Roady and C. A. Sullivan with the plasmajet operation. The critical review of the manuscript by F. M. Bacon is also deeply appreciated. We are particularly indebted to Professor A. J. Barnard, University of British Columbia, for the argon Stark-shift calculations, and to J. Cooper and E. W. Smith, Jr., NBS/Boulder, Colorado, for providing theoretical calculations including ion dynamics at the conditions of this experiment.

---

†This research was supported by the U.S. Atomic Energy Commission.

*This work performed while on sabbatical leave to Sandia Laboratories, Albuquerque, New Mexico 87115.

[1]C. H. Popenoe and J. B. Shumaker, Jr., J. Res. Natl. Bur. Stand. (U.S.) A 69, 495 (1965).

[2]G. P. Petrova, *Studies in Physical Gas Dynamics*, NASA Tech. Transl. TT F-505, 1968 [Issle dovaniya po fizicheskoy gasodinamike (Nauka, Moscow, 1966)].

[3]R. A. Hill and J. B. Gerardo, Phys. Rev. 162, 45 (1967).

[4]J. B. Shumaker and C. H. Popenoe, Phys. Rev. Lett. 21, 1046 (1968).

[5]J. C. Morris and R. U. Krey, Phys. Rev. Lett. 21, 1043 (1968).

[6]W. L. Wiese, D. E. Kelleher, and D. R. Paquette, Phys. Rev. A 6, 1132 (1972).

[7]N. J. Peacock, J. Cooper, and J. R. Greig, Proc. Phys. Soc. Lond. 83, 803 (1964).

[8]D. D. Burgess and C. J. Cairns, J. Phys. B 4, 1364 (1971).

[9]D. D. Burgess and R. Mahon, J. Phys. B 5, 1756 (1972).

[10]C. R. Vidal, J. Cooper, and E. W. Smith, Astrophys. J. Suppl. No. 214, 25, 37 (1973).

[11]P. Kepple and H. R. Griem, Phys. Rev. 173, 317 (1968) [Also see P. Kepple, University of Maryland, Center for Theoretical Physics Report No. 831 (unpublished)].

[12]H. R. Griem, A. C. Kolb, and K. Y. Shen, Astrophys. J. 135, 272 (1962).

[13]G. R. Chester and R. D. Bengtson, University of Texas at Austin (private communication).

[14]The only apparent exceptions to this are Refs. 4 and 5.

[15]The beam splitters used to produce the by-pass beam consisted of dichroic filters that transmit ~90% of the light at 7273 Å and reflect ~85% of the light at 4861 Å at an incidence angle of 45°. They were obtained from the Liberty Mirror Division of Libby-Owens-Ford Glass Co.

[16]D. L. Evans and R. S. Tankin, Phys. Fluids 10, 1136 (1967).

[17]R. W. Porter, SIAM Rev. 6, 228 (1964).

[18]D. L. Evans and J. M. Marchand, Arizona State University, Tempe, Arizona (unpublished).

[19]A. J. Barnard, University of British Columbia, Vancouver, B. C. (private communication).

[20]H. R. Griem, *Plasma Spectroscopy* (McGraw-Hill, New York, 1964).

[21]P. Jacquinot and C. Dufour, J. Rech. Cent. Natl. Rech. Sci., Labs. Bellevue (Paris) No. 6, 91 (1948).

[22]D. P. Aeschliman and R. A. Hill, Appl. Opt. 11, 148 (1972).

[23]D. P. Aeschliman and D. L. Evans (unpublished).

[24]B. D. Adcock, J. Quant. Spectrosc. Radiat. Transfer 7, 385 (1967).

[25]Allowing for the difference in mass between argon atoms and hydrogen atoms, the hydrogen-atom temperature may be expected to be a few percent above the argon-atom temperature. However, since the Doppler width of H_β is small (0.3 Å), the possible error in the convolved profile is negligible. Also, the VCS and KG Stark profiles are very insensitive to T_e; hence, the use of theory for $T_e = 10\,000$ K for data at ~8000 K yields negligible errors in n_e.

[26]We define the term "average percent error over the profile," for N points equally spaced in λ, to be

$$100\left[\ln^{-1}\left(\frac{1}{N}\sum_{i=1}^{N}(\ln j_i^m - \ln j_i^t)^2\right)^{1/2} - 1\right].$$

[27]The atomic-state populations deduced in Ref. 13 were found not to correspond to those normally associated with a thermal distribution, a problem that our plasma does not exhibit. They have concluded that further experimental and theoretical work is needed in order to improve the present understanding of partial local thermodynamic equilibrium in pulsed plasmas. See G. R. Chester, Ph.D. Dissertation (University of Texas at Austin, 1973) (unpublished), available from University Microfilms, Ann Arbor.

[28]D. D. Burgess, A. E. Dangor, and J. E. Jenkins, Brit. J. Appl. Phys. 18, 1281 (1967).

[29]R. A. Hill, J. B. Gerardo, and P. Kepple, Phys. Rev. A 3, 855 (1971).

[30]D. E. Kelleher and W. L. Wiese, Phys. Rev. Lett. 31, 1431 (1973).

[31]J. Cooper, E. W. Smith, and C. R. Vidal, J. Phys. B 7, 101 (1974).

[32]D. P. Aeschliman and A. B. Cambel, Phys. Fluids 13, 2466 (1970).

[33]H. Schlichting, *Boundary Layer Theory* (McGraw-Hill, New York, 1960).

[34]A. Demetriades and E. L. Doughman, J. Plasma Phys. 9, 367 (1973).